Structure and Thermodynamics of Asymmetric Electrolytes Adsorbed in Disordered Electroneutral Charged Matrices from Replica Ornstein−Zernike Equations

Barbara Hribar and Vojko Vlachy

Faculty of Chemistry and Chemical Technology, University of Ljubljana, Ljubljana 1001, Slovenia

Andrij Trokhymchuk† and Orest Pizio*

Instituto de Química de la UNAM, Circuito Exterior, Coyoacán 04510, México D.F.

Received: January 22, 1999

The replica Ornstein−Zernike equations, supplemented by the hypernetted chain approximation, were solved for size and/or charge asymmetric electrolytes adsorbed in a disordered matrix of charged species that are electroneutral in total. More precisely, the matrix was represented as a symmetric +1:−1 electrolyte. To obtain the numerical solution of the replica Ornstein−Zernike equations, renormalization of the initial equations was performed. Both the matrix and adsorbed fluid were modeled as charged hard spheres in a dielectric continuum. As a result of the numerical calculation, we obtained pair distribution functions. The effect of charge and size asymmetry of the annealed fluid was investigated. We present the results for charge asymmetric +2:−1 and +3:−1 electrolytes, and for a solution with asymmetries in charge of +3:−1 (+6:−1) and asymmetries in diameter of 7 Å:4 Å (20 Å:4 Å). In addition to the structural properties, the isothermal compressibility and the excess internal energy of the adsorbed electrolyte were calculated.

1. Introduction

Understanding the thermodynamic and structural properties of fluids adsorbed in a porous material is of importance for basic research and for technology as well. Considerable progress in statistical-mechanical theories for continuum systems with quenched disorder[1−23] has been made in the last decade. Such theoretical research was stimulated by experimental observations indicating that the properties of the adsorbed fluid differ in several aspects from those of the unperturbed bulk fluid.[24−28]

Recently, we began a systematic investigation of partly quenched ionic systems, addressing the problem of screening of Coulombic forces in ionic fluids adsorbed in disordered porous media with charged obstacles.[29,30] In our previous paper,[30] we applied the replica Ornstein−Zernike theory, developed by Given and Stell,[3−5] to study the adsorption of the model ionic fluid in a disordered ionic medium called the matrix. Both the matrix fluid and the adsorbed fluid were treated in the primitive model; i.e., the ions were modeled as charged hard spheres embedded in a dielectric continuum. So far, only symmetric +1:−1 electrolytes with equal-sized ions were considered.[29,30] The replica Ornstein−Zernike (ROZ) equations were solved in the hypernetted chain (HNC) and mean-spherical approximations (MSA) to obtain the pair distribution functions and some thermodynamic parameters.[30] The comparison with published Monte Carlo simulations[22] indicates that both theories yield qualitatively correct predictions for the model under study. As expected from previous studies of bulk electrolytes,[31] the HNC approximation is slightly better in predicting the structural features and excess internal energy of these systems.[30]

Encouraged by these results, we propose an extension of the study to charge and size asymmetric electrolytes. Real electrolytes contain ions of various sizes and valencies. The first deviation from the restricted primitive model of solution is to treat the cations and anions as charged hard spheres of unequal sizes. The differences in size and/or charge cause asymmetry in interaction with charged (or even uncharged) porous material being in contact with the electrolyte solution. This asymmetry may in turn cause unequal distribution of an electrolyte between the bulk solution and porous phase (see for example ref 32) and forms a basis for technological processes of separation. In the model example studied in this paper, the matrix is considered to be a quenched symmetric +1:−1 electrolyte, equilibrated under conditions (temperature, dielectric constant) which are different from the conditions of observation. The annealed (adsorbed) fluid is considered to be (i) a charge asymmetric (+2:−1 and +3:−1) electrolyte, (ii) size asymmetric +1:−1 electrolyte, and for the last part of the calculation, (iii) the charge and size asymmetric electrolyte with asymmetry in charge of +3:−1 (+6:−1) and asymmetry in diameter of 7 Å:4 Å (20 Å:4 Å). The molecular parameters used here do not correspond to any particular electrolyte solution. The diameters of ions are chosen to facilitate the comparison with the previous calculations,[22,29,30,33] but the values are close to the actual diameters of hydrated ions. For example, 20 Å would correspond to a diameter of a small surfactant micelle.

In summary, we are interested in the effects of charge and size of various ionic species on the structural and thermodynamic properties of an adsorbed electrolyte. The numerical results were obtained using the ROZ/HNC approximation (and not for example ROZ/MSA), for this theory is expected to be quite accurate for bulk asymmetric electrolytes.[33,34] The outline of this paper is the following. After this introduction, we present the details of the model (section 2) and of the theoretical procedure used in this study (section 3). The renormalization of ROZ equations is described in section 4. The numerical

* To whom correspondence should be addressed.
† Permanent address: Institute for Condensed Matter Physics, National Academy of Sciences of Ukraine, Lviv 11, Ukraine.

10.1021/jp990253i CCC: $18.00
Published on Web 05/29/1999

results are presented and commented in section 5. Finally, the most important results of this study are summarized in Conclusions.

2. Model System

The model under investigation consists of two components. One is a quenched ionic fluid, which is called the matrix, and the second is an annealed ionic fluid which thermally equilibrates in the presence of matrix species. The notation used in this paper is the same as used before: the superscripts 0 and 1 correspond to the matrix and the annealed fluid species, respectively.[22] The matrix is represented as an electroneutral system of positively and negatively charged hard spheres. The charges of the ions are $ez_+^0 = |ez_-^0| = e$ and their diameters are chosen to be equal, $\sigma_+^0 = \sigma_-^0 = \sigma_0 = 4$ Å. The concentration of matrix particles is ρ_0 ($\rho_+^0 = \rho_-^0 = \rho_0/2$). The matrix ions are immersed in a dielectric continuum with a dielectric constant ϵ_0 and the interaction potential is

$$U_{ij}^{00}(r) = \begin{cases} \infty, & r < \sigma_0 \\ e^2 z_i^0 z_j^0/\epsilon_0 r, & r > \sigma_0 \end{cases} \quad (1)$$

where i and j assume values + and −. The matrix is formed as described: at a certain temperature, T_0, the electrolyte is subjected to a rapid quench. It is assumed that the structure of the fluid does not change during this procedure; the structure of the matrix corresponds to an equilibrium state of an ionic fluid of concentration ρ_0 at temperature T_0. This assumption allows us to use integral equation methods to calculate the pair distribution functions for matrix ions.

The model of the annealed fluid is similar to that of the matrix; it corresponds to an electroneutral system of charged hard spheres with charges ez_+^1 and ez_-^1 and diameters σ_+^1 and σ_-^1. In the present paper four different examples were studied. In the first one, the charge asymmetric electrolytes $z_+ = +2$ or $+3$ and $z_- = -1$, of equal size of ions ($\sigma_+^1 = \sigma_-^1 = 4$ Å) were examined. In the second case we study the size asymmetric electrolyte with $z_+ = +1$ and $z_- = -1$ and of ionic diameters equal to $\sigma_+^1 = 7$ Å and $\sigma_-^1 = 4$ Å. The third case considers the charge and size asymmetric electrolyte with $z_+ = +3$ and $z_- = -1$ and of ionic diameters equal to $\sigma_+^1 = 7$ Å and $\sigma_-^1 = 4$ Å. In the final example we examine the model electrolyte of higher asymmetry in charge and size: $z_+ = +6$ and $z_- = -1$, $\sigma_+^1 = 20$ Å, $\sigma_-^1 = 4$ Å.

The total ionic concentration of annealed species is equal to $\rho_1 = \rho_+^1 + \rho_-^1$. The adsorption is studied at temperature T_1, which is lower than the temperature where the matrix was equilibrated, $T_1 < T_0$. The adsorbing ionic fluid is an electrolyte solution containing ions and solvent. The latter is, in analogy with the matrix subsystem, modeled as a dielectric continuum with constant ϵ. The fluid−fluid and the fluid−matrix interaction potentials are

$$U_{ij}^{11}(r) = \begin{cases} \infty, & r < (\sigma_i^1 + \sigma_j^1)/2 \\ e^2 z_i^1 z_j^1/\epsilon r, & r > (\sigma_i^1 + \sigma_j^1)/2 \end{cases} \quad (2)$$

$$U_{ij}^{10}(r) = U_{ij}^{01}(r) = \begin{cases} \infty, & r < (\sigma_i^1 + \sigma_j^0)/2 \\ e^2 z_i^1 z_j^0/\epsilon r, & r > (\sigma_i^1 + \sigma_j^0)/2 \end{cases} \quad (3)$$

respectively.

3. Theoretical Procedure

The structure and thermodynamics for the model described above can, as proposed before, be obtained by utilizing the replica Ornstein−Zernike equations. The equation for the matrix subsystem reads[30]

$$\mathbf{H}^{00} - \mathbf{C}^{00} = \mathbf{C}^{00} \otimes \boldsymbol{\rho}^0 \mathbf{H}^{00} \quad (4)$$

where $\boldsymbol{\rho}^0$ is a 2 × 2 diagonal matrix with diagonal elements $\rho_+^0 = \rho_-^0 = 0.5\rho_0$ and the symbol ⊗ denotes convolution. The correlation functions in eq 4 are 2 × 2 symmetric matrices with the elements $f_{--}^{00}(r) = f_{++}^{00}(r)$; $f_{+-}^{00}(r) = f_{-+}^{00}(r)$, where f stands for h or c. The ROZ equations for the fluid−matrix and fluid−fluid correlation are

$$\mathbf{H}^{10} - \mathbf{C}^{10} = \mathbf{C}^{10} \otimes \boldsymbol{\rho}^0 \mathbf{H}^{00} + \mathbf{C}^{11} \otimes \boldsymbol{\rho}^1 \mathbf{H}^{10} - \mathbf{C}^{12} \otimes \boldsymbol{\rho}^1 \mathbf{H}^{10}$$

$$\mathbf{H}^{11} - \mathbf{C}^{11} = \mathbf{C}^{10} \otimes \boldsymbol{\rho}^0 \mathbf{H}^{01} + \mathbf{C}^{11} \otimes \boldsymbol{\rho}^1 \mathbf{H}^{11} - \mathbf{C}^{12} \otimes \boldsymbol{\rho}^1 \mathbf{H}^{21}$$

$$\mathbf{H}^{12} - \mathbf{C}^{12} = \mathbf{C}^{10} \otimes \boldsymbol{\rho}^0 \mathbf{H}^{01} + \mathbf{C}^{11} \otimes \boldsymbol{\rho}^1 \mathbf{H}^{12} + \mathbf{C}^{12} \otimes \boldsymbol{\rho}^1 \mathbf{H}^{11} - 2\mathbf{C}^{12} \otimes \boldsymbol{\rho}^1 \mathbf{H}^{21} \quad (5)$$

where, as before, $\boldsymbol{\rho}^1$ is a 2 × 2 diagonal matrix with diagonal elements ρ_+^1 and ρ_-^1. The correlation functions are 2 × 2 matrices with elements $f_{++}(r)$, $f_{+-}(r)$, $f_{-+}(r)$, and $f_{--}(r)$, and each of them consists of connected and blocking parts.[3−5] The connected parts correspond to correlations between particles within the same replica, whereas the blocking parts contain correlation between particles of different replicas. Note that the particles belonging to different replicas do not interact directly—they are correlated due to the presence of the matrix. Functions $\mathbf{H}^{12}$ and $\mathbf{C}^{12}$ represent the blocking contribution to the pair correlation functions and to the direct correlation functions of the annealed fluid (fluid-fluid functions) $\mathbf{H}^{11}$ and $\mathbf{C}^{11}$, respectively.

In order to solve the set of integral equations represented by eqs 5, we need the so-called closure relations. In the present calculation, the ROZ equations were supplemented by the hypernetted chain (HNC) closure. This approximation was found to be very successful in description of bulk symmetric electrolytes,[31] and moderately successful for electrolyte solutions asymmetric in charge and size.[34] On the other hand, the accuracy of the MSA closure deteriorates if asymmetry in charge increases and a rescaling procedure has to be used when this theory is applied to asymmetric electrolytes.[35] The HNC closure was successfully used and tested against the Monte Carlo simulations in our previous study of partly quenched systems.[30]

The HNC closure relations for the replica OZ system of equations read

$$\mathbf{C}^{mn}(r) = \exp[-\beta \mathbf{U}^{mn}(r) + \gamma^{mn}(r)] - 1 - \gamma^{mn}(r)$$

$$\mathbf{C}^{12}(r) = \exp[\gamma^{12}(r)] - 1 - \gamma^{12}(r) \quad (6)$$

where $\gamma^{mn} = \mathbf{H}^{mn} - \mathbf{C}^{mn}$, the superscripts m, n assuming values 0 and 1, and $\mathbf{U}^{mn}$ are the matrices of interparticle interactions for different components.

4. Renormalization of ROZ Equations

In Coulombic systems, the long-range part of the potential requires special treatment. The procedure used for bulk electrolytes has been described in detail in several papers (for example see refs 36 and 37). The renormalization procedure for partly quenched systems was developed and successfully applied in refs 29 and 30. The results presented in this section represent a generalization of our previous calculation.[29] The correlation functions (2 × 2 matrices of h_{ij} or c_{ij} as appropriate)

may be separated into a short-range and a long-range contribution:

$$\mathbf{C}^{mm}(r) = \mathbf{C}^{mm}_{(s)}(r) + \mathbf{\Phi}^{mm}(r)$$

$$\mathbf{C}^{0m}(r) = \mathbf{C}_{(s)}{}^{0m}(r) + \mathbf{\Phi}^{0m}(r)$$

$$\mathbf{C}^{12}(r) = \mathbf{C}^{12}_{(s)}(r) \quad (7)$$

$$\mathbf{H}^{mn}(r) = \mathbf{H}^{mn}_{(s)}(r) + \mathbf{q}^{mn}(r) \quad (8)$$

where the superscripts m, n assume the values 0,1,2. Further, $\mathbf{C}^{22}(r) = \mathbf{C}^{11}(r)$, $\mathbf{C}^{01}(r) = \mathbf{C}^{02}(r)$, $\mathbf{H}^{22}(r) = \mathbf{H}^{11}(r)$; $\mathbf{\Phi}^{22}(r) = \mathbf{\Phi}^{11}(r)$. Considering that the particles belonging to different replicas do not interact, we put $\mathbf{\Phi}^{12}(r) = \mathbf{0}$. We choose the elements $\varphi^{mn}_{ij}(r)$ of the matrix $\mathbf{\Phi}^{mn}(r)$ in the form of the Coulomb interactions:

$$\varphi^{mn}_{ij}(r) = -e^2 z_i^m z_j^n / k_B \epsilon T_1 r$$

$$\varphi^{00}_{ij}(r) = -e^2 z_i^0 z_j^0 / k_B \epsilon_0 T_0 r \quad (9)$$

where k_B is the Boltzmann constant, while functions $\mathbf{q}^{mn}(r)$ are chosen to satisfy the following equations (10)

$$\mathbf{q}^{00} - \mathbf{\Phi}^{00} = \mathbf{\Phi}^{00} \otimes \boldsymbol{\rho}^0 \mathbf{q}^{00}$$

$$\mathbf{q}^{10} - \mathbf{\Phi}^{10} = \mathbf{\Phi}^{10} \otimes \boldsymbol{\rho}^0 \mathbf{q}^{00} + \mathbf{\Phi}^{11} \otimes \boldsymbol{\rho}^1 \mathbf{q}^{10}$$

$$\mathbf{q}^{11} - \mathbf{\Phi}^{11} = \mathbf{\Phi}^{10} \otimes \boldsymbol{\rho}^0 \mathbf{q}^{01} + \mathbf{\Phi}^{11} \otimes \boldsymbol{\rho}^1 \mathbf{q}^{11}$$

$$\mathbf{q}^{12} - \mathbf{\Phi}^{12} = \mathbf{\Phi}^{10} \otimes \boldsymbol{\rho}^0 \mathbf{q}^{01} + \mathbf{\Phi}^{11} \otimes \boldsymbol{\rho}^1 \mathbf{q}^{12} \quad (10)$$

The elements $\mathbf{q}^{mn}_{ij}(r)$ of the matrices $\mathbf{q}^{mn}$ assume the Debye−Hückel-like form:

$$\begin{pmatrix} q^{00}_{++}(r) & q^{00}_{+-}(r) \\ q^{00}_{+-}(r) & q^{00}_{--}(r) \end{pmatrix} = -L_B/Q \begin{pmatrix} z^0_+ z^0_+ & z^0_+ z^0_- \\ z^0_+ z^0_- & z^0_- z^0_- \end{pmatrix} \frac{\exp(-\kappa_0 r)}{r}$$

$$\begin{pmatrix} q^{10}_{++}(r) & q^{10}_{+-}(r) \\ q^{10}_{-+}(r) & q^{10}_{--}(r) \end{pmatrix} = -L_B \frac{\kappa_0^2}{\kappa_0^2 - \kappa_1^2} \begin{pmatrix} z^1_+ z^0_+ & z^1_+ z^0_- \\ z^1_- z^0_+ & z^1_- z^0_- \end{pmatrix} \times \left[\frac{\exp(-\kappa_0 r)}{r} - \frac{\kappa_1^2}{\kappa_0^2} \frac{\exp(-\kappa_1 r)}{r} \right]$$

$$\begin{pmatrix} q^{12}_{++}(r) & q^{12}_{+-}(r) \\ q^{12}_{+-}(r) & q^{12}_{--}(r) \end{pmatrix} = 2\pi L_B^2 \frac{\rho^0_+ (z^0_+)^2 + \rho^+_- (z^0_-)^2}{\kappa_0^2 - \kappa_1^2} \times \left\{ \frac{-2\kappa_0^2 \exp(-\kappa_0 r)}{r(\kappa_0^2 - \kappa_1^2)} + \frac{2\kappa_0^2 \exp(-\kappa_1 r)}{r(\kappa_0^2 - \kappa_1^2)} - \kappa_1 \exp(-\kappa_1 r) \right\} \times \begin{pmatrix} z^1_+ z^1_+ & z^1_+ z^1_- \\ z^1_- z^1_+ & z^1_- z^1_- \end{pmatrix}$$

$$\begin{pmatrix} q^{11}_{++}(r) & q^{11}_{+-}(r) \\ q^{11}_{+-}(r) & q^{11}_{--}(r) \end{pmatrix} = -L_B \begin{pmatrix} z^1_+ z^1_+ & z^1_+ z^1_- \\ z^1_+ z^1_- & z^1_- z^1_- \end{pmatrix} \frac{\exp(-\kappa_1 r)}{r} + \begin{pmatrix} q^{12}_{++}(r) & q^{12}_{+-}(r) \\ q^{12}_{+-}(r) & q^{12}_{--}(r) \end{pmatrix} \quad (11)$$

where $\kappa_0 = (4\pi \sum \rho_i^0 (z_i^0)^2 L_B/Q)^{1/2}$, $\kappa_1 = (4\pi \sum \rho_i^1 (z_i^1)^2 L_B)^{1/2}$, and $L_B = e^2/k_B \epsilon T_1 = 7.14$ Å.

Finally, the ROZ equations are rewritten in a renormalized form. First, we present the equation for the matrix subsystem:

$$\mathbf{H}^{00}_{(s)} - \mathbf{C}^{00}_{(s)} = \mathbf{C}^{00}_{(s)} \otimes \boldsymbol{\rho}^0 (\mathbf{H}^{00}_{(s)} + \mathbf{q}^{00}) + \mathbf{\Phi}^{00} \otimes \boldsymbol{\rho}^0 \mathbf{H}_{(s)}{}^{00} \quad (12)$$

and continue with

$$\mathbf{H}^{10}_{(s)} - \mathbf{C}^{10}_{(s)} = \mathbf{C}^{10}_{(s)} \otimes \boldsymbol{\rho}^0 (\mathbf{H}^{00}_{(s)} + \mathbf{q}^{00}) + \mathbf{\Phi}^{10} \otimes \boldsymbol{\rho}^0 \mathbf{H}^{00}_{(s)} + \mathbf{C}^{11}_{(s)} \otimes \boldsymbol{\rho}^1 (\mathbf{H}^{10}_{(s)} + \mathbf{q}^{10}) + \mathbf{\Phi}^{11} \otimes \boldsymbol{\rho}^1 \mathbf{H}^{10}_{(s)} - \mathbf{C}^{12}_{(s)} \otimes \boldsymbol{\rho}^1 (\mathbf{H}^{10}_{(s)} + \mathbf{q}^{10})$$

$$\mathbf{H}^{11}_{(s)} - \mathbf{C}^{11}_{(s)} = \mathbf{C}^{10}_{(s)} \otimes \boldsymbol{\rho}^0 (\mathbf{H}^{01}_{(s)} + \mathbf{q}^{01}) + \mathbf{\Phi}^{10} \otimes \boldsymbol{\rho}^0 \mathbf{H}^{01}_{(s)} + \mathbf{C}_{(s)}{}^{11} \otimes \boldsymbol{\rho}^1 (\mathbf{H}^{11}_{(s)} + \mathbf{q}^{11}) + \mathbf{\Phi}^{11} \otimes \boldsymbol{\rho}^1 \mathbf{H}^{11}_{(s)} - \mathbf{C}^{12}_{(s)} \otimes \boldsymbol{\rho}^1 (\mathbf{H}^{21}_{(s)} + \mathbf{q}^{21})$$

$$\mathbf{H}^{12}_{(s)} - \mathbf{C}^{12}_{(s)} = \mathbf{C}^{10}_{(s)} \otimes \boldsymbol{\rho}^0 (\mathbf{H}^{01}_{(s)} + \mathbf{q}^{01}) + \mathbf{\Phi}^{10} \otimes \boldsymbol{\rho}^0 \mathbf{H}^{01}_{(s)} + \mathbf{C}^{11}_{(s)} \otimes \boldsymbol{\rho}^1 (\mathbf{H}^{12}_{(s)} + \mathbf{q}^{12}) + \mathbf{\Phi}^{11} \otimes \boldsymbol{\rho}^1 \mathbf{H}^{12}_{(s)} + \mathbf{C}^{12}_{(s)} \otimes \boldsymbol{\rho}^1 \mathbf{H}^{11} - 2\mathbf{C}^{12}_{(s)} \otimes \boldsymbol{\rho}^1 \mathbf{H}^{21} \quad (13)$$

The ROZ equations presented above were solved numerically by a direct iteration over $N = 16\,384$ points for the majority of the calculations. The integration step Δr varied from 0.05 to 0.08 Å, depending on the ionic valencies and concentration. A large number of integration points was needed because the interactions are of long range (especially for dilute solutions) and at the same time $g(r)$'s are rapidly varying functions near the multivalent ions. The second reason for the large N is a convergence problem; we have to stress that the convergence rate for the asymmetric electrolytes is considerably lower than that for the symmetric +1:−1 solutions studied before.[30]

We shall conclude this section with equations for thermodynamic properties which can be calculated once the distribution functions are known. The excess internal energy of a charged fluid inside a charged matrix ($\beta = 1/k_B T_1$) can be calculated from eq 14:[14]

$$\beta E^{ex}/N^1 = {}^1/_2 \sum_{i=+,-} \sum_{j=+,-} x_i^1 \rho_j^1 \int \mathrm{d}\mathbf{r}\, g^{11}_{ij}(r) U^{11}_{ij}(r) + \sum_{i=+,-} \sum_{j=+,-} x_i^1 \rho_j^0 \int \mathrm{d}\mathbf{r}\, g^{10}_{ij}(r) U^{10}_{ij}(r) \quad (14)$$

Another well-established relation is the equation[8] which reads

$$\beta \frac{\partial P}{\partial \rho_1} = 1 - \rho_1 \sum_{i=+,-} \sum_{i=+,-} x_i^1 x_j^1 \int \mathrm{d}\mathbf{r}\, [C^{11}_{(s)ij}(r) - C^{12}_{(s)ij}(r)] \quad (15)$$

Note that the reduced compressibility presented in Tables 1−3 and discussed in text is actually an inverse of eq 15.

One quantity that is of considerable interest in electrochemistry is the excess chemical potential. For bulk electrolyte solutions there are several ways to calculate this quantity; one route has been proposed by Rasaiah and Friedman[38] via the composition fluctuation formula. Yet another approach, valid within the HNC and related integral equation theories, has been proposed by Kjellander and Sarman.[39] On the other hand, in the case of the ROZ formalism there is presently no general route to calculate this quantity.[5] We are currently exploring the

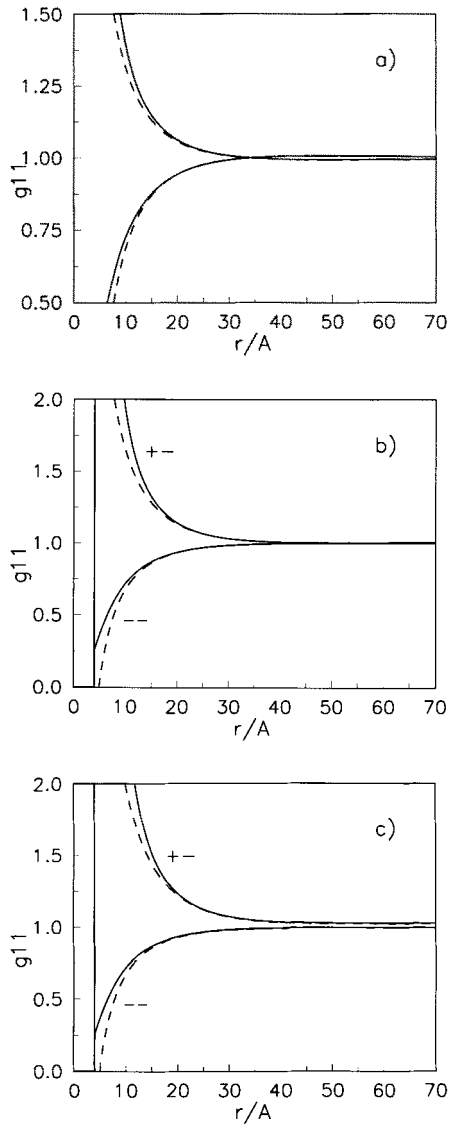

Figure 1. Annealed fluid ion−ion pair distribution functions in the ROZ-HNC approximation, $g^{11}_{+-}(r)$, and $g^{11}_{--}(r)$ (solid lines) and their counterparts with long-range asymptotic terms, $1 + q^{11}_{+-}(r)$ and $1 + q^{11}_{--}(r)$ (dashed lines). The calculations apply to the following values of parameters: $c^0 = 0.05$ M, quenching parameter $Q = 1.2$, $\sigma^1_- = \sigma^1_+ = 4$ Å, $c^1_+ = 0.0001$ M, (a) $z^1_+ + 1$, (b) $z^1_+ = +2$, (c) $z^1_+ = +3$; $z^1_- = -1$ in all calculations.

possibility of adaptation of formula proposed in ref 38 and we hope to report the numerical results in one of the future papers.

5. Results and Discussion

We begin the discussion with the results for charge asymmetric electrolytes with equal sized ions, adsorbed in the matrix represented by a symmetric +1:−1 electrolyte. The temperature of observation is $T_1 = 298$ K and the so-called quenching parameter is $Q = \epsilon_0 T_0/\epsilon T_1 = 1.2$ in all calculations presented in this paper. First we studied the model electrolyte with $\sigma^1_+ = \sigma^1_- = 4$ Å, $z^1_- = -1$ and for (a) $z^1_+ = +1$ (symmetric case), (b) $z^1_+ = +2$, and (c) $z^1_+ = +3$. The symmetric case a has been examined in some detail before,[30] and the results for +1:−1 annealed fluid are presented here for the sake of comparison with examples b and c.

The results for a matrix concentration $c^0 = 0.05$ mol dm^{-3} are shown in Figures 1 and 2. In Figure 1a we present an example where the concentration of the annealed fluid is very

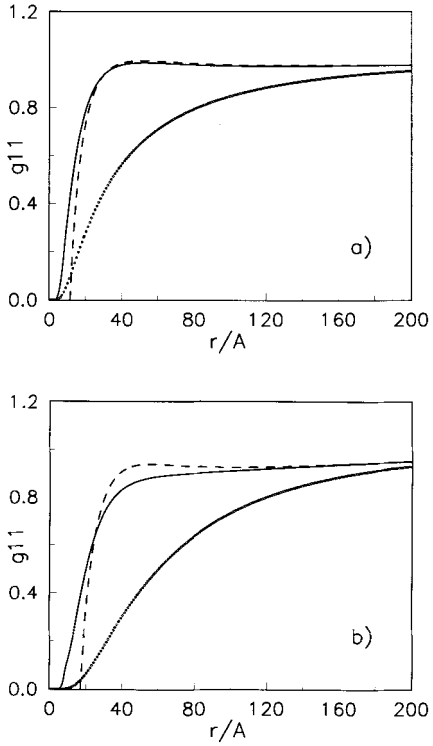

Figure 2. Same as for Figure 1, but for $g^{11}_{++}(r)$ (solid line) and its counterpart with long-range asymptotic term, $1 + q^{11}_{++}(r)$ (dashed line); the symbols represent the pair distribution functions of a pure electrolyte: (a) $z^1_+ = +2$, (b) $z^1_+ = +3$; other values of parameters as before.

low compared to the concentration of matrix ions ($c^1_+ = 10^{-4}$ mol dm^{-3}). Both the cations and anions of the annealed fluid are monovalent in this case. The influence of the matrix ions on the structure of the adsorbed fluid is strong enough here to cause the crossover of ++ and +− pair distribution functions as shown in Figure 1a. The conclusion is that there is a range of distances where equally charged ions attract each other while, on the other hand, there is a repulsion between oppositely charged fluid ions. This effect was first noticed in the computer simulations of Bratko and Chakraborty[22] and later reproduced by the ROZ studies.[29,30] The crossover is due to the presence of matrix ions and is a long-range effect, for it is seen in the q functions too. Note again that Figure 1a applies to the symmetric +1:−1 electrolyte adsorbed in the matrix fluid containing monovalent (+1:−1) ions.

For charge asymmetric electrolytes we have, due to asymmetry, three different distribution functions. In Figure 1b we present the −− and +− distribution functions for a +2:−1 electrolyte adsorbed in the matrix, while Figure 1c shows the corresponding functions for a +3:−1 electrolyte. As the charge asymmetry between the fluid cations and anions increases, the pair distribution functions between the monovalent anions change the shape—there is no crossing point seen for these two cases (cf. Figure 1, b and c). There is a strong correlation between the positive and negative ions—the peaks of the distribution functions, which are offscale in the figures, assume values of 3.9, 14.7, and 51.4 for Figure 1, a, b, and c, respectively. The corresponding ++ (multivalent cations) pair distribution functions are shown in Figure 2, together with the function for the bulk (unperturbed) electrolyte, presented by the symbols. Note that, in comparison with the bulk fluid, the correlations among the fluid ions in the matrix are of much shorter range.

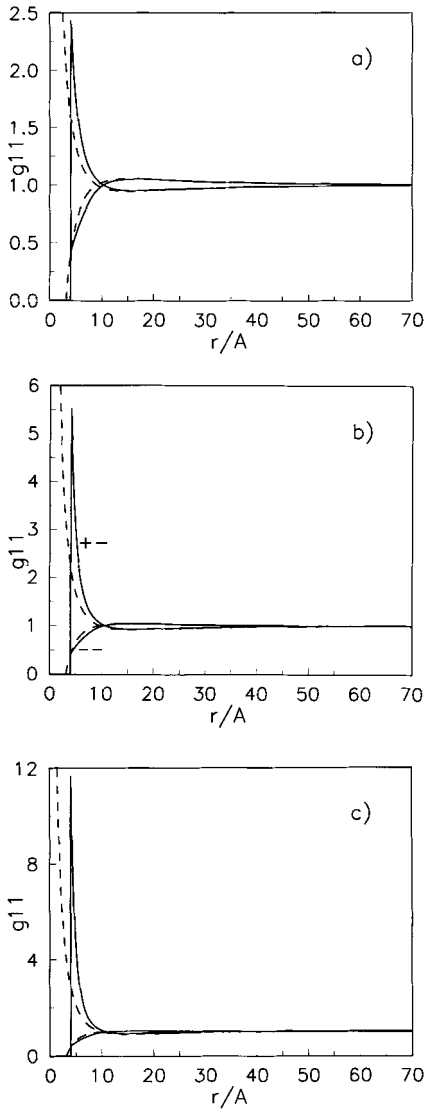

Figure 3. Same as for Figure 1, but at matrix concentration $c^0 = 0.5$ M.

At a higher matrix concentration, $c^0 = 0.5$ mol dm^{-3}, presented in Figure 3, we clearly observe the crossover of the $+-$ and $--$ pair correlation functions. Again Figure 3a shows the correlation for a symmetric $+1{:}-1$ annealed fluid. In Figure 3, b and c, the charge asymmetric cases $+2{:}-1$ and $+3{:}-1$ are presented, respectively. As we see, for divalent and trivalent ions double crossing of the pair distribution functions occurs. In other words, there is a region between the two crossing points, within which the interaction between the like ions is attractive. This region is smaller as the valence of the cations increases from $+2$ to $+3$. The effect seems to be a consequence of an interplay of blocking and connected contributions to screening between the electrolyte ions.

The pair distribution functions between multivalent cations are shown in Figure 4, a and b. In this figure also the corresponding functions of the bulk electrolyte at the same concentration are shown. The g^{11}_{++} function shown in Figure 4a exhibits a peak, which is unusual for the strongly repulsive force acting between divalent ions. The peak is due to the influence of matrix. Interestingly, in the next figure (Figure 4b), representing the corresponding function for trivalent cations, this peak disappears. This is probably due to a stronger direct interaction between the trivalent ions. In both examples, the effect of the matrix is to make the correlation between the multivalent ions

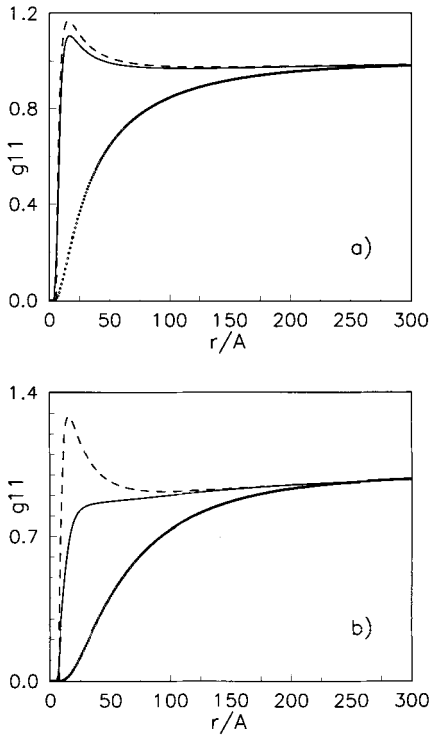

Figure 4. Same as for Figure 2, but at matrix concentration $c^0 = 0.5$ M.

of shorter range, in comparison with the unperturbed (bulk) electrolyte under the same conditions.

In the second part of this paper we consider systems where the ions of annealed fluid differ in charge and size. The matrix fluid is, as before, modeled as a symmetric $+1{:}-1$ electrolyte. For the case presented next, the size and charge of the cations $\sigma^1_+ = 7$ Å, and (a) $z^1_+ = +1$ or (b) $z^1_+ = +3$ were chosen. In the second example examined here we present a system of a greater asymmetry in size and charge, with $z^1_+ = +6$ and $\sigma^1_+ = 20$ Å. In both cases the counterions were monovalent and they have the same diameter as before, $\sigma^1_- = 4$ Å. One problem encountered during the study of such charge and size asymmetric electrolytes is the poor convergence of the replica Ornstein−Zernike equations. This is not totally unexpected, for the convergence of integral equations is difficult to obtain for solutions of bulk asymmetric electrolytes as well.[33,40] So the absence of the convergence may not necessarily have a physical significance; for example, we have reached a limit of adsorption. The parameters chosen here were therefore, to a certain degree, dictated by the convergency problems. That is, for higher asymmetry in size and charge, the convergence is extremely slow. The structural properties, as given by various distribution function, are shown in Figures 5−8.

The results shown in Figure 5 were obtained for a matrix concentration $c^0 = 0.05$ mol dm^{-3} and for concentration of the adsorbed electrolyte $c^1_+ = 0.0001$ mol dm^{-3}. In this calculation the cation and anion of the annealed electrolyte solution differ in size: $\sigma^1_+ = 7$ Å and $\sigma^1_- = 4$ Å. Two different cases were studied: Figure 5a presents results for charge symmetric $+1{:}-1$ electrolyte, while in Figure 5b we show the calculation for $+3{:}-1$ annealed electrolyte. The contact values for the $+-$ distribution functions (not shown in Figure 5, a and b) are 2.4 and 5.8, respectively. These figures, when compared with the results displayed in Figure 1, a and c, illustrate the effects of the size asymmetry.

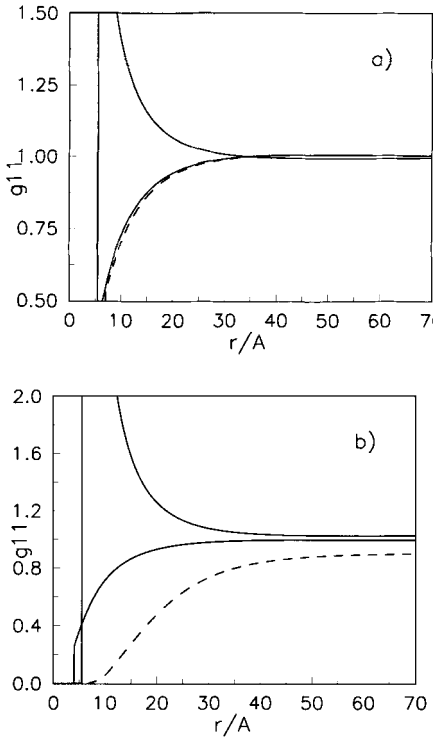

Figure 5. Annealed fluid ion−ion pair distribution functions in the ROZ-HNC approximation, $g^{11}_{+-}(r)$, $g^{11}_{--}(r)$ (solid lines) and $g^{11}_{++}(r)$ (dashed lines). The calculations apply to: $c^0 = 0.05$ M, $c^1_+ = 0.0001$ M, $Q = 1.2$, $\sigma^1_+ = 7$ Å, $\sigma_-{}^1 = 4$ Å, $z^1_- = -1$; (a) $z^1_+ = +1$, and (b) $z^1_+ = +3$.

Figures 6−8 display the results for a +6:−1 annealed electrolyte in a matrix formed by a symmetric +1:−1 electrolyte of concentration $c^0 = 0.05$ mol dm^{-3}. The calculations apply to $c^1_+ = 10^{-5}$ mol dm^{-3}, $z^1_+ = +6$, and for a diameter of the macroion $\sigma^1_+ = 20$ Å. First, in Figure 6, we show the annealed fluid ion−ion pair distribution functions for (a) ++, (b) +−, and (c) −− pairs of ions. The corresponding functions for the bulk asymmetric electrolyte are shown on the same figures by symbols. One effect produced by the presence of matrix ions is a better screening of the interionic correlation. For the counterion−counterion (−−) pair distribution function, shown in Figure 6c, we observe a peak not present in the bulk electrolyte of this concentration. The peak in the counterion−counterion distribution function, here induced by the matrix, is normally present in bulk asymmetric electrolytes of higher asymmetry in charge.[33,34]

Figure 7 presents the annealed fluid pair distribution functions for the same case as described above (Figure 6), but at a higher fluid concentration $c^1_+ = 0.05$ mol dm^{-3}. For this case, the concentration of the annealed electrolyte is equal to the concentration of the matrix ions and the effect of the matrix ions is very small here. The corresponding distribution functions for the bulk asymmetric electrolyte lie almost exactly on top of the distribution functions for the annealed electrolyte in Figure 7.

In the next figure (Figure 8) we investigated the effect of varying the concentration of the annealed fluid on the fluid−matrix correlation. The parameters used in this calculation are the same as for Figure 7, except for the concentration of the annealed fluid. First, in Figure 8a, the annealed fluid−matrix pair distribution functions for $c^1_+ = 10^{-5}$ mol dm^{-3} are shown. Strong accumulation of the annealed fluid ions around the oppositely charged matrix ions is shown in Figure 8. The

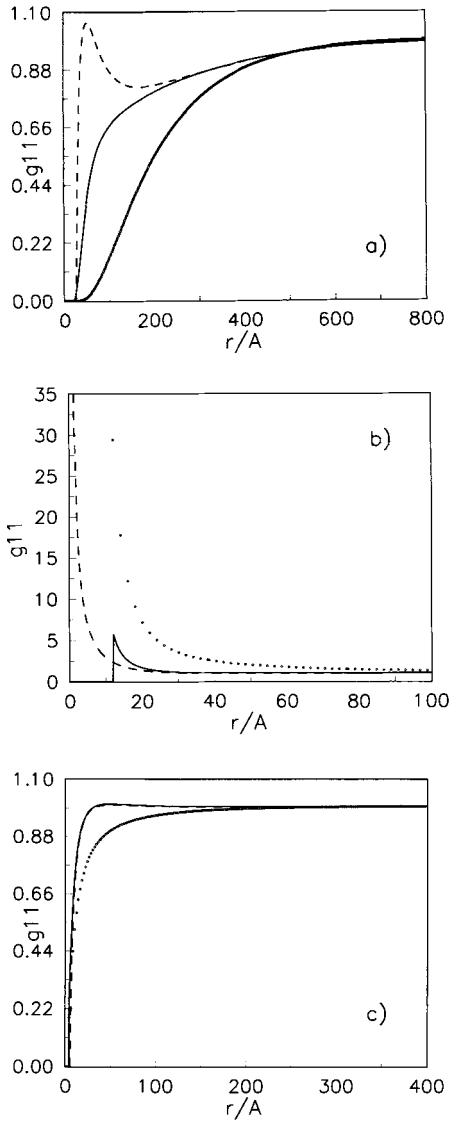

Figure 6. Annealed fluid ion−ion pair distribution functions in the ROZ-HNC approximation (a) $g^{11}_{++}(r)$, (b) $g^{11}_{+-}(r)$, and (c) $g^{11}_{--}(r)$, (solid lines) and their counterparts with long-range asymptotic terms, $1 + q^{11}_{++}(r)$, $1 + q_{+-}{}^{11}(r)$, and $1 + q^{11}_{--}(r)$ (dashed lines). The symbols represent pair distribution functions of a pure fluid. The calculations apply to the following values of parameters: $c^0 = 0.05$ M, quenching parameter $Q = 1.2$, $z^1_+ = +6$ and $\sigma^1_+ = 20$ Å; $c^1_+ = 10^{-5}$ M.

nonmonotonic behavior of the like-pair distribution functions (−− and ++) between the annealed and matrix ions in the case of Figure 8b are due to the combination of excluded volume and Coulombic effects.

In some of the figures presented so far, the results for the long-range functions, $1 + q^{11}_{ij}$, are shown. While these functions are needed in numerical solution of ROZ equations (see section 4), they are interesting per se. The q functions, namely, are obtained using the theory which corresponds to the Debye−Hückel approximation (or the MSA theory for pointlike ions) for bulk electrolyte solutions.[29] The analytical results presented in section 4 (cf. eq 11) are generalization of the previously derived equations[29] and are valid for arbitrary asymmetry in charge. In this respect we should mention that the approximations involved in the calculations of q functions limit their validity to low concentrations and to solutions with pointlike ions. Nevertheless, the q functions (long-range part of the pair distribution functions) yield qualitatively correct description (for all distances r) of ionic distributions in several cases (cf. Figures

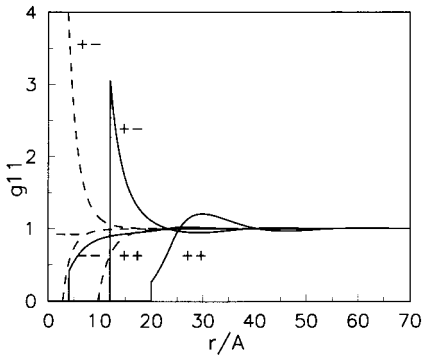

Figure 7. Annealed fluid ion−ion pair distribution functions in the ROZ-HNC approximation $g^{11}_{++}(r)$, $g^{11}_{+-}(r)$, and $g^{11}_{--}(r)$ (solid lines), and their counterparts with long-range asymptotic terms, $1 + q^{11}_{++}(r)$, $1 + q^{11}_{+-}(r)$, and $1 + q^{11}_{--}(r)$ (dashed lines). The calculations apply to the following values of parameters: $c^0 = 0.05$ M, quenching parameter, $Q = 1.2$, $z^1_+ = +6$, and $\sigma^1_+ = 20$ Å; $c^1_+ = 0.05$ M.

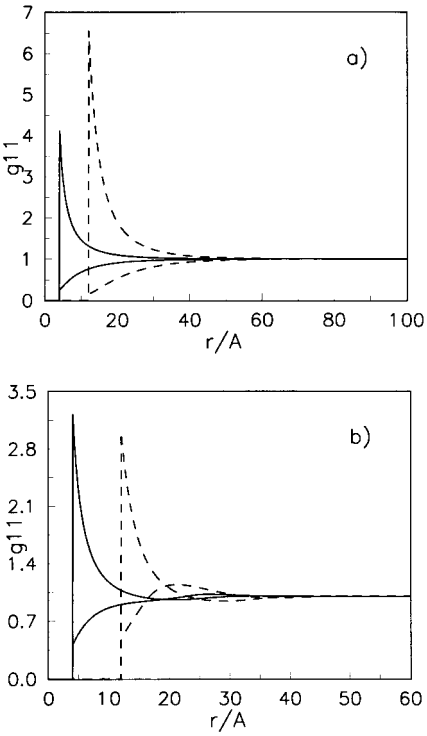

Figure 8. Annealed fluid−matrix pair distribution functions in the ROZ-HNC approximation, $g^{10}_{++}(r)$ and $g^{10}_{+-}(r)$, (dashed lines), and $g^{10}_{--}(r)$ and $g^{10}_{-+}(r)$ (solid lines). The calculations apply to: $c^0 = 0.05$ M, $Q = 1.2$, $z^1_+ = +6$, and $\sigma^1_+ = 20$ Å; $c^1_+ =$ (a) 10^{-5} M and (b) 0.05 M.

1−3 and 4a) where no asymmetry in size is involved. In all these cases, we believe, the MSA closure would also yield a satisfactory description of the interionic correlation. For strong couplings (cf. Figure 4b) or for solutions containing large multivalent ions (Figures 6 and 7), the *q* functions, as expected, fail to describe small *r* behavior correctly.

The thermodynamic properties for three different concentrations of matrix ions are collected in Tables 1−3. All calculations apply to $Q = 1.2$ and the concentration of the annealed electrolyte was varied over relatively broad limits. In Table 1 the results for $c^0 = 0.005$ mol dm^{-3} are presented; for this value the influence of the matrix is very small, except for the lowest concentration of the annealed electrolyte. In Table 2 we present the results for $c^0 = 0.05$ mol dm^{-3} and in Table 3 for $c^0 = 0.5$ mol dm^{-3}; the last results apply to charge asymmetric, but otherwise equally-sized ions of adsorbed fluid. The reduced quantity defined in captions to tables to be $\beta^{-1}(\partial\rho^1/\partial P)$ represents the ratio of the compressibility of the fluid and the compressibility of ideal gas and it is for bulk electrolytes studied in ref 41.

TABLE 1: Excess Internal Energy, $-E^{ex}/N^1kT$, and the Compressibility, $\beta^{-1}(\partial\rho^1/\partial P)$, of a Charged Hard Sphere Fluid in a Charged Hard Sphere Matrix at $Q = 1.2$ and at Different Fluid Concentrations[a]

z^1_+	σ^1_+ (Å)	c^1_+ (M)	$-E^{ex}/N^1kT$	$\beta^{-1}(\partial\rho^1/\partial P)$
+1	4	0.0001	0.1540	0.9996
		0.005	0.1426	1.0058
		0.1	0.2901	1.0293
+2		0.0001	0.3099	0.9992
		0.005	0.3598	1.0288
		0.1	0.8267	1.1210
+3		0.0001	0.5246	0.9993
		0.005	0.7064	1.0514
		0.1	1.5037	1.2213
	7	0.0001	0.4512	1.0003
		0.005	0.5827	1.0628
		0.1	1.2227	1.3410
+6	20	0.00001	0.829	1.000
		0.0001	0.704	1.001
		0.001	0.771	1.004
		0.005	1.011	1.014
		0.05	1.545	1.078

[a] Matrix concentration is $c^0 = 0.005$ M.

TABLE 2: Excess Internal Energy, $-E^{ex}/N^1kT$, and the Compressibility, $\beta^{-1}(\partial\rho^1/\partial P)$, of a Charged Hard Sphere Fluid in a Charged Hard Sphere Matrix at $Q = 1.2$ and at Different Fluid Concentrations[a]

z^1_+	σ^1_+ (Å)	c^1_+ (M)	$-E^{ex}/N^1kT$	$\beta^{-1}(\partial\rho^1/\partial P)$
+1	4	0.0001	0.4499	0.9991
		0.005	0.3751	1.0007
		0.1	0.3806	1.0247
	7	0.0001	0.4290	0.9991
		0.005	0.3542	1.0004
		0.1	0.3475	1.0090
+2	4	0.0001	0.9318	0.9949
		0.005	0.7510	1.0088
		0.1	0.9296	1.1098
+3		0.0001	1.5210	0.9880
		0.005	1.2041	1.0192
		0.1	1.6086	1.2048
	7	0.0001	1.2764	0.9896
		0.005	1.0051	1.0312
		0.1	1.3123	1.3202
+6	20	0.00001	1.925	0.999
		0.0001	1.654	0.999
		0.001	1.376	1.003
		0.005	1.339	1.013
		0.05	1.635	1.071

[a] Matrix concentration is $c^0 = 0.05$ M.

The trends observed in Tables 1−3 are as follows: both the excess internal energy and the reduced compressibility decrease on increasing the concentration of matrix fluid. The effect of matrix concentration on the reduced compressibility is small at relatively low matrix densities (from $c^0 = 0.005$ mol dm^{-3} to $c^0 = 0.5$ mol dm^{-3}) studied here. Due to the correlation with matrix ions, the concentration fluctuations are suppressed, and the compressibility of annealed electrolyte decreases with the increasing concentration of matrix ions. This parallels the behavior of electrolyte solution within the charged capillary.[32] The data for the excess internal energy indicate that this quantity depends on the concentration of the annealed electrolyte in a complex way, depending on the valencies of ions and on the matrix density. In most cases it decreases with an increasing

TABLE 3: Excess Internal Energy, $-E^{ex}/N^1kT$, and the Compressibility, $\beta^{-1}(\partial\rho^1/\partial P)$, of a Charged Hard Sphere Fluid in a Charged Hard Sphere Matrix at $Q = 1.2$ and at Different Fluid Concentrations[a]

z_+^1	σ_+^1 (Å)	c_+^1 (M)	$-E^{ex}/N^1kT$	$\beta^{-1}(\partial\rho^1/\partial P)$
+1	4	0.0001	1.0370	0.9990
		0.005	0.9271	0.9958
		0.1	0.7312	1.0103
+2		0.0001	2.1019	0.9926
		0.005	1.7552	0.9880
		0.1	1.4058	1.0719
+3		0.0001	3.2382	0.9850
		0.005	2.5492	0.9940
		0.1	2.1337	1.1512

[a] Matrix concentration is $c^0 = 0.5$ M.

concentration of the annealed electrolyte, but there are examples, where the excess internal energy is a nonmonotonic function of c_+^1. Note, however, that the results presented in Tables 1−3 apply to low concentrations of the annealed electrolyte, starting from from $c_+^1 = 0.0001$ mol dm^{-3} to $c_+^1 = 0.1$ mol dm^{-3}. In all cases studied here, the reduced compressibility increases with increasing concentration of annealed fluid; the same holds true for bulk electrolytes at low concentrations.[41]

6. Conclusions

In this paper we are concerned with the influence of the charge and size of ions forming the annealed electrolyte, distributed within the electroneutral matrix with ionic obstacles. For all calculations the matrix is represented as a symmetric (−1:+1) electrolyte with ions of equal size. To obtain the numerical solution of the replica Ornstein−Zernike equations in the hypernetted-chain approximation, renormalization of the original equations was performed. As a result of the calculation we present the pair distribution functions and thermodynamic properties such as the excess internal energy and isothermal compressibility.

In the first part of the study we considered a charge symmetric (+1:−1) and a charge asymmetric (+2:−1 and +3:−1) annealed electrolyte adsorbed in a +1:−1 matrix electrolyte. The two electrolytes are treated in the primitive model approximation—all the ions have equal size and the solvent is considered as a dielectric continuum with the properties of water. The results for distribution functions in +2:−1 and +3:−1 electrolytes are similar to those obtained for symmetric +1:−1 electrolytes (see also refs 29 and 30). For a sufficiently high ratio of matrix to annealed fluid concentration, we observe crossover behavior of the −− and +− fluid ion distribution functions. This is a long-range effect due to the matrix ions and has been observed in computer simulations as well.[22] Multivalent cations make this effect smaller as seen in Figure 3 of the present paper. Of considerable interest is to compare the structure of the annealed fluid with that of the unperturbed bulk electrolyte. The pair distribution functions are substantially modified under the influence of matrix ions, if the latter are present in sufficient concentration. One effect is to make the interionic correlation between the multivalent like-charge ions of shorter range. One particularly interesting result is a peak in the +2:+2 distribution function, not present in the bulk electrolyte under these conditions. The results for charge and size asymmetric electrolytes, distributed in the +1:−1 matrix of equally-sized ions, are even more complex—they depend on charge and size of the present ionic species. As the size of the ions of annealed electrolyte increases and/or at higher concentrations, the hard core interactions start to play more important role in shaping the ionic distributions.

This calculation considers a more realistic model of the annealed electrolyte solution than studied before;[22,29,30] the electrolyte is modeled as a mixture of charged hard spheres of different sizes and charges embedded in continuous dielectric. The model system is characterized by a large number of parameters and in this calculation we have varied only few of them. In particular, it remains to investigate the influence of the matrix preparation, i.e., to extend the calculation to other values of the quenching parameter Q. Further, it is of considerable interest to investigate electrolyte solutions of higher asymmetry in charge and size than studied here. One obstacle in the way to these extensions is the rather poor convergence of the numerical procedure. We believe that the theory could be improved in the same spirit as previously proposed for bulk asymmetric electrolytes.[33,42] In one of the future studies we shall also explore partially quenched systems, where the matrix is formed by a charge and size asymmetric electrolyte. The influence of the matrix on the thermodynamic and structural properties of the adsorbed electrolyte (symmetric or asymmetric) is expected to be stronger in such a case. The model system may be of interest for polyelectrolyte science, for it resembles dense polyelectrolyte solutions.

Acknowledgment. This work was supported in part by DGAPA of the UNAM under research grant IN 111597 and by CONACyT of Mexico under grant No. 25301-E. B.H. is grateful to the Slovenian Science Foundation for financial support during her stay at UNAM. B.H. and V.V. acknowledge the support of the Slovene Ministry of Science and Technology.

References and Notes

(1) Madden, W. G.; Glandt, E. D. *J. Stat. Phys.* **1988**, *51*, 537.
(2) Madden, W. G. *J. Chem. Phys.* **1992**, *96*, 5422; **1995**, *102*, 5572.
(3) Given, J. A.; Stell, G. *J. Chem. Phys.* **1992**, *97*, 4573.
(4) Given, J. A.; Stell, G. *Physica A* **1994**, *209*, 495.
(5) Given, J. A. *J. Chem. Phys.* **1995**, *102*, 2934.
(6) Lomba, E.; Given, J. A.; Stell, G.; Weis, J. J.; Levesque D. *Phys. Rev. E* **1993**, *48*, 233.
(7) Fanti, L. A.; Glandt, E. D.; Madden, W. G. *J. Chem. Phys.* **1990**, *93*, 5945.
(8) Rosinberg, M. L.; Tarjus, G.; Stell, G. *J. Chem. Phys.* **1994**, *100*, 5172.
(9) Meroni, A.; Levesque, D.; Weis, J. J. *J. Chem. Phys.* **1996**, *105*, 1101.
(10) Kaminsky, R. D.; Monson, P. A. *J. Chem. Phys.* **1991**, *95*, 2936.
(11) Vega, C.; Kaminsky, R. D.; Monson, P. A. *J. Chem. Phys.* **1993**, *99*, 3003.
(12) Ford, D. M.; Glandt, E. D. *J. Chem. Phys.* **1994**, *100*, 2392.
(13) Trokhymchuk, A. D.; Pizio, O.; Holovko, M. F.; Sokolowski, S. *J. Phys. Chem.* **1996**, *100*, 17004.
(14) Kierlik, E.; Rosinberg, M. L.; Tarjus, G.; Monson, P. A. *J. Chem. Phys.* **1997**, *106*, 264.
(15) Pitard, E.; Rosinberg, M. L.; Stell, G.; Tarjus, G. *Phys. Rev. Lett.* **1995**, *74*, 4361.
(16) Bratko, D.; Chakraborty, A. K. *Phys. Rev. E* **1995**, *51*, 5805.
(17) Chakraborty, A. K.; Bratko, D.; Chandler, D. *J. Chem. Phys.* **1994**, *100*, 1528.
(18) Wu, D.; Hui, K.; Chandler, D. *J. Chem. Phys.* **1992**, *96*, 835.
(19) Deem, M. W.; Chandler, D. *J. Stat. Phys.* **1994**, *76*, 907.
(20) Leung, K.; Chandler, D. *J. Chem. Phys.* **1995**, *102*, 1405.
(21) Gordon, P. A.; Glandt, E. D. *J. Chem. Phys.* **1996**, *105*, 4257.
(22) Bratko, D.; Chakraborty, A. K. *J. Chem. Phys.* **1996**, *104*, 7700.
(23) Muthukumar, M. *J. Chem. Phys.* **1989**, **1989**, *90*, 4594.
(24) Wong, A. P. Y.; Chan, M. H. W. *Phys. Rev. Lett.* **1990**, *65*, 2567.
(25) Frisken, B. J.; Cannell, D. S. *Phys. Rev. Lett.* **1992**, *69*, 632.
(26) Goh, M. C.; Goldburg, W. I.; Knobler, C. M. *Phys. Rev. Lett.* **1987**, **1987**, *58*, 1008.
(27) Maher, J. V.; Goldburg, W. I.; Pohl, D. W.; Lanz, M. *Phys. Rev. Lett.* **1984**, *53*, 60.
(28) Wong, A. P. Y.; Kim, S. B.; Goldburg, W. I.; Chan, M. H. W. *Phys. Rev. Lett.* **1993**, *70*, 954.

(29) Hribar, B.; Pizio, O.; Trokhymchuk, A.; Vlachy, V. *J. Chem. Phys.* **1997**, *107*, 6335.
(30) Hribar, B.; Pizio, O.; Trokhymchuk, A.; Vlachy, V. *J. Chem. Phys.* **1998**, *109*, 2480.
(31) Rasaiah, J. C. In *The Liquid state and its Electrical Properties*; Kunhardt, E. E., Christophorou, L. G., Luessen, H. L., Eds.; NATO ASI Series B 193; Plenum: New York, 1988.
(32) Jamnik, B.; Vlachy, V. *J. Am. Chem. Soc.* **1993**, *115*, 660.
(33) Hribar, B.; Krienke, H.; Kalyuzhnyi, Yu. V.; Vlachy, V. *J. Mol. Liq.* **1997**, *73*,*74*, 277.
(34) Vlachy, V.; Marshall, C. H.; Haymet, A. D. J. *J. Am. Chem. Soc.* **1989**, *111*, 4160.
(35) Sheu, E.; Wu, C. F.; Chen, S. H.; Blum, L. *Phys. Rev. A* **1985**, *32*, 3807.
(36) Duh, D. M.; Haymet, A. D. J. *J. Chem. Phys.* **1992**, *97*, 7716.
(37) Ichiye, T.; Haymet, A. D. J. *J. Chem. Phys.* **1990**, *93*, 8954.
(38) Rasaiah, J. C.; Friedman, H. L. *J. Chem. Phys.* **1968**, *48*, 2742.
(39) Kjellander, R.; Sarman, S. *J. Chem. Phys.* **1989**, *90*, 2768.
(40) Belloni, L. *Phys. Rev. Lett.* **1986**, *57*, 2026.
(41) Vlachy, V.; Ichiye, T.; Haymet, A. D. J. *J. Am. Chem. Soc.* **1991**, *113*, 1077.
(42) Kalyuzhnyi, Y. V.; Vlachy, V. *Chem. Phys. Lett.* **1993**, *215*, 518.